J. Am. Chem. Soc. 1990, 112, 2498-2506

A New Series of Amphiphilic Molecules Forming Stable Z-Type (Polar) Langmuir–Blodgett Films

R. Popovitz-Biro,[*,†] K. Hill,[†,⊥] E. Shavit,[†] D. J. Hung,[†] M. Lahav,[†] L. Leiserowitz,[†] J. Sagiv,[‡] H. Hsiung,[§] G. R. Meredith,[§] and H. Vanherzeele[§]

Contribution from the Department of Structural Chemistry and Department of Isotope Research, The Weizmann Institute of Science, Rehovot 76100, Israel, and Central Research and Development, E. I. Du Pont de Nemours & Company, Wilmington, Delaware 19880.
Received August 14, 1989

Abstract: A new series of amphiphilic molecules bearing two amide groups along the hydrocarbon chain form head-to-tail Z-type (polar) multilayers by the Langmuir–Blodgett (LB) technique, in contrast with the common amphiphiles that tend to deposit in the head-to-head, tail-to-tail Y-type fashion. Molecules with one amide group along the chain form Y-type or Z-type structures, depending on the location of the amide along the chain. *p*-Nitroaniline or merocyanine groups could be aligned in a polar sense, by attaching them covalently to such amphiphiles, to yield multilayers displaying second-harmonic generation (SHG). These films were characterized by ellipsometric, X-ray diffraction, IR, UV, and SHG measurements. The Z-type deposition correlates with the observed low water contact angles of the films, indicating formation of porous structures in which water may penetrate. This behavior is rationalized in terms of the hydrophilic nature of the amide groups that retain water by hydrogen bonding. In keeping with this mechanism, it was anticipated that amphiphiles bearing other polar groups, such as hydroxyls along the hydrocarbon chain, also form Z-type LB films.

The Langmuir–Blodgett (LB) technique has recently aroused considerable interest as a method for buildup of ordered multilayers of amphiphilic molecules. This renaissance has been inspired from the many potential technological applications of such films.[1] In particular, polar multilayers are expected to show pyroelectric, piezoelectric, and nonlinear optical effects, as a result of constructive summation of dipoles and hyperpolarizability tensors.[2]

The most common and thermodynamically stable multilayer structures are of the Y-type, where the layers are deposited in a head-to-head, tail-to-tail fashion.[3] Polar Y-type films, of the general ABAB··· arrangement, can be prepared by alternate deposition of A and B, with special two-compartment troughs[4] (Chart I).

Z-Type multilayers, comprised of molecules of the same kind in a head-to-tail arrangement, are formed when deposition onto the solid substrate occurs only during the upstroke of the dipping cycle. In certain cases, Z-type structures could be obtained by decompression[5,2c] or removal[6] of the monolayer from the air/water interface prior to the down stroke. Several sporadic examples of genuine Z-type depositions have been previously reported: a cyanoalkylterphenyl system,[7] a double-chain fluorocarbon,[8] an anthracene derivative,[9] and several polymeric systems.[10,11] From these examples it would be difficult to make any generalizations or predictions as to which amphiphiles would tend to deposit in a polar structure. Therefore in order to design polar LB films, an understanding of deposition behavior on a molecular level is required.

The deposition behavior is determined by the shape of the water meniscus during deposition, as controlled by the wettability (advancing and receding contact angles) of the previously deposited layer. The hydrophilic character of the exposed surface in the various types of films increases in the order X < Y < Z.[12a] If the surface is strongly hydrophobic, both advancing and receding contact angles are >90°. In such a case, deposition occurs only during dipping of the substrate, but no on withdrawal (X-type).[12b] If the surface is less hydrophobic such that the advancing contact angle is >90° and the receding contact angle is <90°, deposition will occur on both dipping and withdrawal (Y-type). Z-Type multilayers are formed when deposition occurs only during withdrawal. Such behavior requires both advancing and receding contact angles to be <90° (Chart II).

Chart I

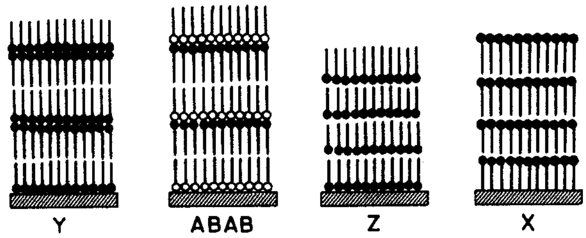

Chart II

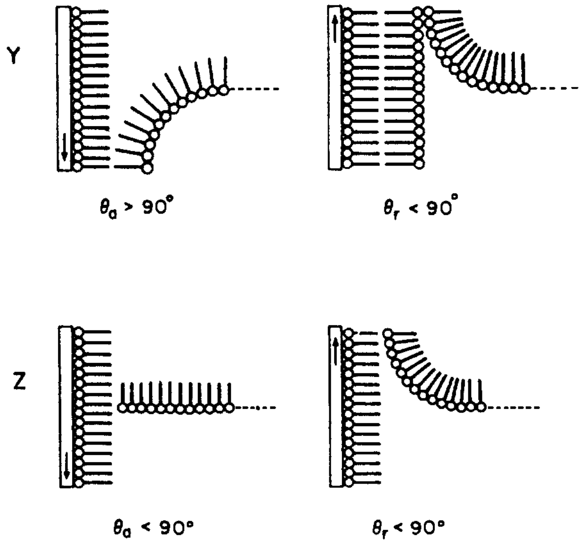

Design of polar Z-type films requires a means to increase the hydrophilicity of the surface but without use of bipolar amphiphiles that may induce bent conformations or mixtures of two different orientations at the air/water interface. Moreover, for applications

---

[†] Department of Structural Chemistry, The Weizmann Institute of Science.
[‡] Department of Isotope Research, The Weizmann Institute of Science.
[§] E. I. Du Pont de Nemours & Co.
[⊥] Present address: Henkel Research Corp., Santa Rosa, CA 95407.

(1) (a) Swalen, D. J.; Allara, D. L.; Andrade, J. D.; Chandross, E. A.; Garoff, S.; Israelachvili, J.; McCarthy, T. J.; Murray, R.; Pease, R. F.; Rabolt, J. F.; Wynne, K. J.; Yu, H. *Langmuir* **1987**, *3*, 932. (b) Sugi, M. J. *Mol. Electron.* **1985**, *1*, 3.

(2) (a) Blinov, L. M.; Dubinin, N. V; Mikhnev, L. V.; Yudin, S. G. *Thin Solid Films* **1984**, *120*, 161. (b) Girling, I. R.; Kolinsky, P. V.; Cade, N. A.; Earls, J. D.; Peterson, I. R. *Optics Commun.* **1985**, *55*, 289. (c) Richardson, T.; Roberts, G. G.; Polywka, M. E. C.; Davies, S. G. *Thin Solid Films* **1988**, *160*, 231.

(3) (a) Fendler, J. H. *Membrane Mimetic Chemistry*; John Wiley and Sons: New York, 1982. (b) Gaines, G. L., Jr. *Insoluble Monolayers at Liquid-Gas Interfaces*; Interscience: New York, 1966.

0002-7863/90/1512-2498$02.50/0

Table I

class no.	no.	compound	multilayer type	contact angle advancing (receding)
I	**1**	$CH_3(CH_2)_{14}C(O)NH(CH_2)_4CH(NH_3^+)CO_2^-$	Z	80 (24)
	2	$CH_3(CH_2)_{14}C(O)NH(CH_2)_3CH(NH_3^+)CO_2^-$	Y	100 (45)
	3	$CH_3(CH_2)_{14}C(O)NH(CH_2)_2CH(NH_3^+)CO_2^-$	Y	92 (39)
	4	$CH_3(CH_2)_{17}NHC(O)(CH_2)_2CH(NH_3^+)CO_2^-$	Y	94 (18)
	5	$CH_3(CH_2)_{17}NHC(O)CH_2CH(NH_3^+)CO_2^-$	Y	93 (36)
	6	$CH_3(CH_2)_9C(O)NH(CH_2)_{11}CO_2H$	Z	85 (30)
	7	$CH_3(CH_2)_9C(O)NH(CH_2)_{11}CONH_2$	Z	80 (25)
	8	$CH_3(CH_2)_9C(O)O(CH_2)_{11}C(O)NH(CH_2)_4CH(NH_3^+)CO_2^-$	Z	70 (22)
II	**9**	$CH_3(CH_2)_9C(O)O(CH_2)_{11}CO_2H$	Y	88 (35)
	10	$CH_3(CH_2)_{17}OC(O)(CH_2)_2CH(NH_3^+)CO_2^-$	Y	95 (40)
	11	$CH_3(CH_2)_{17}OC(O)CH_2CH(NH_3^+)CO_2^-$	Y	95 (45)
III	**12**	$CH_3(CH_2)_9C(O)NH(CH_2)_{11}C(O)NH(CH_2)_4CH(NH_3^+)CO_2^-$	Z	75 (15)
	13	$CH_3(CH_2)_{10}C(O)NH(CH_2)_{10}C(O)NH(CH_2)_4CH(NH_3^+)CO_2^-$	Z	82 (28)
	14	$CH_3(CH_2)_{10}C(O)NH(CH_2)_{10}C(O)NH(CH_2)_3CH(NH_3^+)CO_2^-$	Z	80 (25)
	15	$Br(CH_2)_{10}C(O)NH(CH_2)_{11}C(O)NH(CH_2)_4CH(NH_3^+)CO_2^-$	Z	70 (10)
IV	**16**	$p\text{-}O_2NC_6H_4NH(CH_2)_{11}C(O)NH(CH_2)_{11}C(O)NH(CH_2)_4CH(NH_3^+)CO_2^-$	Z	70 (40)
	17	$p\text{-}O_2NC_6H_4NH(CH_2)_{11}C(O)NH(CH_2)_{11}C(O)NH(CH_2)_3CH(NH_3^+)CO_2^-$	Z	72 (30)
	18	$p\text{-}O_2NC_6H_4CH{=}CHC(O)NH(CH_2)_{11}C(O)NH(CH_2)_4CH(NH_3^+)CO_2^-$	Z	64 (10)
	19	$O{=}C_6H_4{=}C_2H_2{=}C_5H_4N(CH_2)_{10}C(O)NH(CH_2)_{11}CO_2^-K^+$	Z	68 (45)
	20	$CH_3(CH_2)_4NHC(O)(CH_2)_{11}NHC(O)(CH_2)_{10}NC_5H_4{=}C_2H_2{=}C_6H_4{=}O$	Z	75 (30)
	21	$p\text{-}O_2NC_6H_4NH(CH_2)_{11}C(O)NH(CH_2)_{11}CO_2H$		
	22	$CH_3(CH_2)_{11}NHC(O)(CH_2)_{11}NH\text{-}p\text{-}O_2NC_6H_4$		
V	**23**	$CH_3(CH_2)_{15}C{\equiv}CC{\equiv}C(CH_2)_8C(O)NH(CH_2)_4CH(NH_3^+)CO_2^-$	Z	89 (37)
	24	$CH_3(CH_2)_{15}C{\equiv}CC{\equiv}C(CH_2)_8C(O)NH(CH_2)_3CH(NH_3^+)CO_2^-$	Z	90 (25)

in the field of nonlinear optics, the ω-position of the hydrocarbon chain should be free for the attachment of various groups with high hyperpolarizabilities.

Wettability is a macroscopic property that has not been treated theoretically on a molecular scale.[13] Experiments have demonstrated that this property is determined by the structure and polarity of groups close to the interface.[14] Wettability has also been found to depend on porosity of the film to water.[15] However, in certain cases groups with strong dipoles located as much as 10 Å underneath the surface show an effect on wettability.[16] Hydratable polar groups incorporated beneath the surface may influence molecular packing, as well as water penetration and retention in the film, without being part of the outermost region of the surface.[17a]

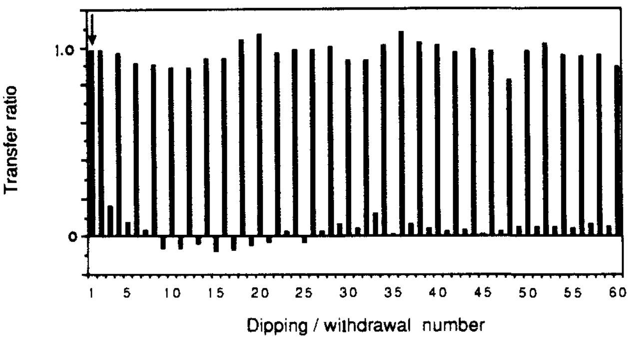

Figure 1. Histogram showing the apparent transfer ratio of a monolayer of **14** on hydrophobic glass slide.

During a previous study on crystal nucleation by Langmuir and Langmuir–Blodgett films,[18] we synthesized various amphiphiles by coupling amino acids to long-chain carboxylic acids via an ester or amide linkage. We observed that palmitoyl-(*S*)-lysine (**1**) (Table I) gave Z-type deposition at 20 mN/m while palmitoyl-(*S*)-ornithine (**2**), having the amide group closer to the head group by only one methylene, formed the regular Y-type multilayer under the same conditions. These observations served as a point of departure for the design of amphiphiles bearing various polar groups along the hydrocarbon chain that might form Z-type multilayers. In particular, we investigated the role played by these polar groups on water retention and wettability of the resulting films and, thereby, on their deposition behavior.

---

(4) (a) Ledoux, I.; Josse, D.; Fremaux, P.; Zyss, J.; McLean, T.; Hann, R. A.; Gordon, P. F.; Allen, S. *Thin Solid Films* **1988**, *160*, 217. (b) Smith, G. W.; Daniel, M. F.; Barton, J. W.; Ratcliffe, N. *Thin Solid Films* **1985**, *132*, 125. (c) Girling, I. E.; Cade, N. A.; Kolinsky, P. V.; Earls, J. D.; Cross, G. H.; Peterson, I. R. *Thin Solid Films* **1985**, *132*, 101. (d) Barraud, A.; Leloup, J.; Gauzern, A.; Palacin, S. *Thin Solid Films* **1985**, *133*, 117. (e) Daniel, M. F.; Dolphin, J. C.; Grant, A. J.; Kerr, K. E. N.; Smith, G. W. *Thin Solid Films* **1985**, *133*, 235.

(5) (a) Kalina, D. W.; Grubb, S. G. *Thin Solid Films* **1988**, *160*, 363. (b) Richardson, T.; Roberts, G. G.; Polywka, M. E. C.; Davies, S. G.; *Thin Solid Films* **1988**, *160*, 231. (c) Loulerque, J. C.; Doumont, M.; Levy, Y.; Robin, P.; Pocholle, J. P.; Papouchon, M. *Thin Solid Films* **1988**, *160*, 399.

(6) Blinov, L. M.; Davydova, N. N.; Lazareva, V. T.; Yudin, S. G. *Sov. Phys. Solid State* (*Engl. Transl.*) **1982**, *24*, 1523.

(7) Daniel, M. F.; Lettington, O. C.; Small, S. M. *Thin Solid Films* **1983**, *99*, 61.

(8) Higashi, N.; Kunitake, T. *Chem. Lett.* **1986**, 105.

(9) Vincett, P. S.; Barlow, W. A.; Boyle, F. T.; Finney, J. A. *Thin Solid Films* **1979**, *60*, 265.

(10) Winter, C. S.; Tredgold, R. H. *Thin Solid Films* **1985**, *123*, L1.

(11) (a) Mumby, S. J.; Swalen, J. D.; Rabolt, J. F. *Macromolecules* **1986**, *19*, 1054. (b) Stroeve, P.; Srinivasan, M. P.; Higgins, B. G.; Kowel, S. T. *Thin Solid Films* **1987**, *146*, 209.

(12) (a) Bikerman, J. J. *Proc. R. Soc. London, A.* **1939**, *170*, 130. (b) Cemel, A.; Tomlinson Fort, Jr.; Lando, J. *J. Polym. Sci. Part A-1*, **1972**, *10*, 2061.

(13) (a) Joanny, J. F.; de Gennes, P. G., *J. Chem. Phys.* **1984**, *81*, 552. (b) Schwartz, L. W.; Garoff, S. *Langmuir* **1985**, *1*, 219.

(14) (a) Zisman, W. A. In *Contact Angle, Wettability and Adhesion*; Fowkes, F. M., Ed.; Advances in Chemistry Series 43; American Chemical Society: Wasington DC, 1964. (b) Traughton, E. B.; Bain, C. D.; Whitesides, G. M.; Nuzzo, R. G.; Allara, D.; Porter, M. D. *Langmuir* **1988**, *4*, 365. (c) Davies, J. T.; Rideal, E. K. *Interfacial Phenomena*; Academic Press: New York and London, 1963. (d) Jaycock, M. J.; Parfitt, G. D. *Chemistry of Interfaces*; Ellis Horwood: Chichester, 1981. (e) Good, R. J.; Stromberg, R. R. *Surface and Colloid Science*; Plenum: New York, 1979; Vol. 2.

(15) (a) Bain, C. D.; Whitesides, G. M. *J. Am. Chem. Soc.* **1988**, *110*, 5897. (b) Maoz, R.; Sagiv, J. *Langmuir* **1987**, *3*, 1034. (c) Maoz, R.; Sagiv, J. *Langmuir* **1987**, *3*, 1045.

(16) Shafrin, E. G.; Zisman, W. A. *J. Phys. Chem.* **1962**, *66*, 740.

(17) (a) Popovitz-Biro, R.; Hill, K.; Landau, E. M.; Lahav, M.; Leiserowitz, L.; Sagiv, J.; Hsiung, H.; Meredith, G. R.; Vanherzeele, H. *J. Am. Chem. Soc.* **1988**, *110*, 2672. (b) Popovitz-Biro, R.; Hung, D. J.; Shavit, E.; Lahav, M.; Leiserowitz, L. *Thin Solid Films* **1989**, *178*, 203.

(18) (a) Landau, E. M.; Grayer Wolf, S.; Levanon, M.; Leiserowitz, L.; Lahav, M.; Sagiv, J. *J. Am. Chem. Soc.* **1989**, *111*, 1436. (b) Landau, E. M.; Grayer Wolf, S.; Sagiv, J.; Deutsch, M.; Kjaer, K.; AlsNielsen, J.; Leiserowitz, L.; Lahav, M. *Pure Appl. Chem.* **1989**, *61*, 673.

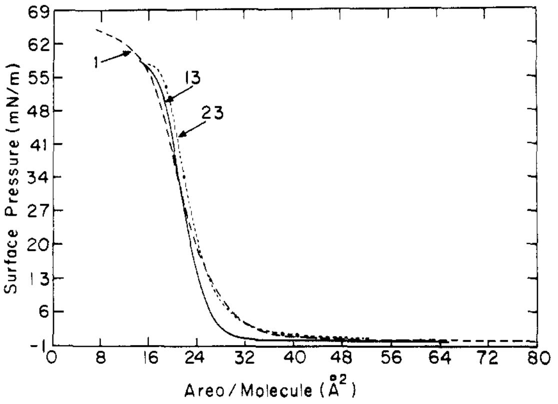

Figure 2. Pressure–area isotherms of **1**, **13**, and **23** over pure water at 20 °C.

Results

Amphiphilic molecules bearing α-amino acid, carboxylic acid, merocyanine, or *p*-nitroaniline head groups and hydrocarbon chains incorporating polar groups as amides, alcohols, esters, ketones, and polymerizable diacetylenes were synthesized; their deposition behavior was studied and related to wettability properties.

Table I lists the amphiphilic molecules, their transfer behavior at 20 mN/m, and contact angles with water (advancing and receding). The amphiphiles are classified according to the type and number of functional groups incorporated in the hydrocarbon chains. Representative examples of the resulting multilayers were characterized by IR (reflection–absorption), UV, ellipsometry, X-ray, and second-harmonic generation (SHG) measurements.

Class I includes amphiphiles with amino acid, carboxylic acid, or amide head groups and hydrocarbon chains 20–29 atoms long, bearing one amide at various positions. Both Y- and Z-type multilayers were obtained with amphiphiles in this group, depending on the location of the amide group along the chain. An amide placed only one to three methylenes from the head group yielded the regular Y-type multilayer. On the other hand, when the amide group was located four or more methylenes from the head group, the advancing contact angle with water was lower than 90° and Z-type multilayers were obtained.

When ester groups were incorporated at various positions along the hydrocarbon chain, Y-type multilayers were obtained under the same conditions (class II).

Incorporation of a second amide group into a hydrocarbon chain has an effect on wettability and deposition behavior similar to that of moving the amide further apart from the head group. Compounds in this class (III) are amphiphiles with amino acid head groups and a hydrocarbon chain of 29–31 atoms, bearing two amides, one located at least nine methylenes away from the terminal methyl group and the second three or four methylenes from the amino acid moiety. It is noteworthy that the amphiphiles with two amide groups *in* the chain are decidedly more stable at the air/water interface than those with one amide group, as observed by good transfer ratios for large number of dipping cycles. Up to 50 layers of compound **14** were deposited on hydrophilic or hydrophobic (treated with octadecyltrichlorosilane OTS) glass slides (Figure 1) without any deterioration in transfer behavior observed. When deposition was made onto hydrophobic glass slides, the first two layers were a Y-type bilayer and the successive layers were Z-type. This behavior is general for all amphiphiles that give Z-type deposition on hydrophilic slides.

Attachment of various groups with high hyperpolarizabilities, such as *p*-nitroaniline or merocyanine, at the end of amphiphiles with two amides along the hydrocarbon chain did not alter their Z-type mode of deposition (see Table I, class IV). Consequently, multilayers of such amphiphiles showed frequency doubling via second-harmonic generation, thus providing independent proof of their polar structure.

With the aim of increasing the film stability, we synthesized amphiphiles having one amide group and a diacetylene polymerizable function. Monolayers of diacetylenic carboxylic acids have been extensively studied,[19] all forming the usual Y-type multilayers. Compounds **23** and **24** were synthesized by coupling 10,12-nonacosadiynoic acid with (*S*)-lysine and (*S*)-ornithine, respectively. Monolayers of monomers and polymers of these amphiphiles could be deposited as Z-type films.[17b]

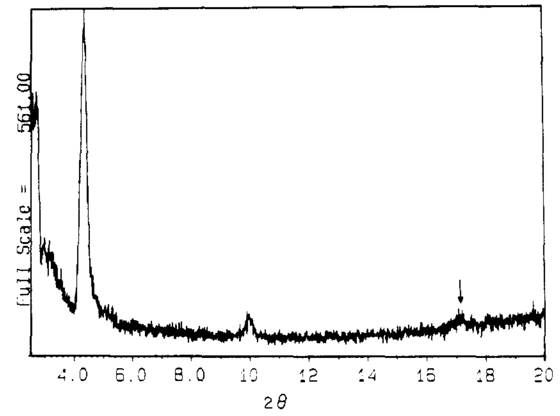

Figure 3. Low-angle X-ray diffraction pattern of 10 layers of **14** deposited on hydrophobic glass.

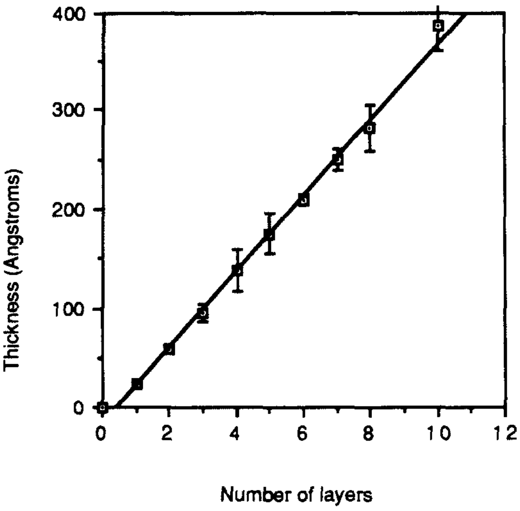

Figure 4. Film thickness (by ellipsometry) of **14** as function of the number of deposited layers.

Pressure–Area Isotherms. Figure 2 shows the Π–A isotherms of compounds **1**, **13**, and **23** as representative examples. Π–A isotherms of all the amphiphiles have been measured at 20 °C on double-distilled water at neutral pH. Amphiphiles in class I–III and V all form condensed monolayers with a relatively steep rise in the pressure at the transition from expanded to condensed phase. The limiting molecular areas are 27–29 Å² for amphiphiles with amino acid head groups and 20–25 Å² for amphiphiles with carboxylic acid or amide head groups. Several amphiphiles in class IV show transition between expanded and condensed films that appear as a plateau of nearly constant pressure.

Layer Spacing Determination by Ellipsometry and X-rays. In order to exclude the possibility that any rearrangement of the deposited films occurred following the deposition procedure, the layer spacings of several of these multilayers were determined by low-angle X-ray diffraction (Cu Kα, λ = 1.54 Å) and by ellipsometry. Multilayer samples, with 10, 17, 43, and 49 layers of compound **14** on glass slides, were measured by X-rays. All samples gave two diffraction peaks at 2θ = 4.3° and 10°, and in some spectra a third peak was observed at 17.2°, corresponding to the (002), (005), and (008) reflections (Figure 3). A layer spacing of 42 ± 1.6 Å was calculated from the above spectra.

---

(19) (a) Leiser, G.; Tieke, B.; Wegner, G. *Thin Solid Films* **1980**, *68*, 77. (b) Day, D.; Lando, J. B. *Macromolecules* **1980**, *13*, 1478. (c) Day, D.; Hub, H. H.; Ringsdorf, H. *Isr. J. Chem.* **1979**, *18*, 325.

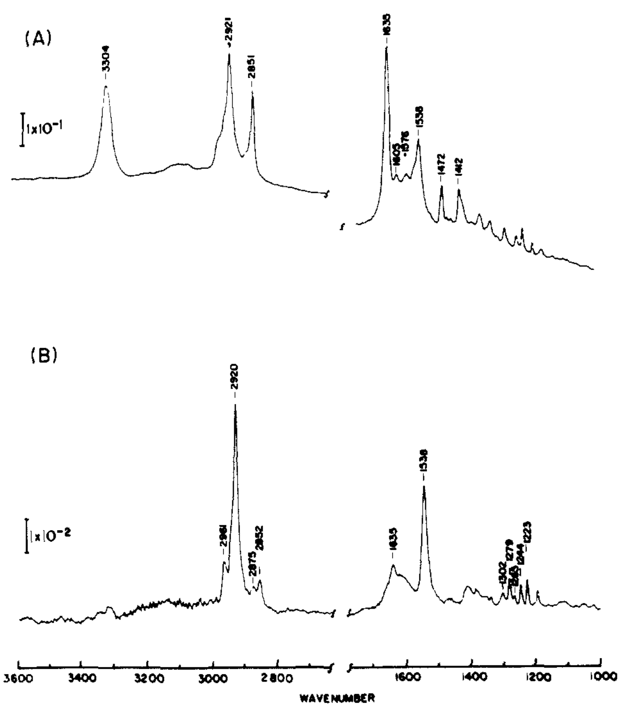

Figure 5. IR spectra of **14**: (A) in the bulk (KBr pellet), measured in transmission mode; (B) in LB film (10 layers) on gold-coated glass, measured in reflection mode.

Multilayers of **14** were also prepared on glass slides coated with evaporated gold. The film thickness was measured by ellipsometry after each dipping cycle, up to 10 cycles. The plot of film thickness vs the number of layers yielded a straight line (Figure 4). The layer spacing obtained from the slope of the above is 39 ± 3 Å, which is in reasonable agreement with the X-ray data. A layer spacing of approximately 40 Å is consistent with a head-to-tail Z-type structure, requiring a tilt of about 20° relative to the surface normal, whereas a Y-type packing would lead to a spacing of almost double that value. Similarly, ellipsometric measurements on samples of 2–12 layers of **13** gave an average layer spacing of 38.5 ± 3 Å. The calculated molecular length in the extended conformation is 43.6 Å; thus, the observed spacing requires a tilt of approximately 28° relative to the surface normal.[20]

Multilayer samples of 30 layers of compound **17** measured by low-angle X-ray diffraction gave very weak peaks at $2\theta = 4.0°$ and 6.3°, corresponding to the (002) and (003) reflections. The layer spacing calculated therefrom was 43 ± 1 Å. X-ray data of 13 polymeric layers of **23** showed three Bragg peaks at $2\theta = 3.7°$, 5.8°, and 8.3°, corresponding to a characteristic spacing of 45.3 ± 2.6 Å. This value is consistent with a Z-type head-to-tail relation of the layers in the film, requiring a tilt of approximately 25° relative to the surface normal. Ellipsometric measurements on samples of 5 and 10 layers of the monomer gave an average layer spacing of 47 ± 2 Å, which is in good agreement with the X-ray data.

Infrared Spectroscopy. Multilayers deposited on gold-coated glass were also characterized by FT-IR in the reflection absorption mode, with p-polarized light, which gives preferential selection to polarization components perpendicular to the surface.[21a] Comparison of the relative intensities of bands in these spectra with those measured in transmission mode for the bulk material can provide information about the orientation of certain groups in the molecules comprising the LB films. For example, such a comparison for compound **14** is shown in Figure 5. Examination of the 2800–3000-cm^{-1} region shows that in the multilayer spectrum the asymmetric and symmetric CH_3 stretching bands at 2961 and 2875 cm^{-1} are of comparable intensity to the symmetric CH_2 stretching band at 2852 cm^{-1}, whereas the asymmetric CH_2 band at 2920 cm^{-1} is relatively more intense than in the bulk. These differences may be interpreted in terms of a large deviation of the chain axis from the surface normal in the direction perpendicular to the chain backbone.[21b] A tilt of the molecular axis, relative to the surface normal, is also consistent with the X-ray and ellipsometric measurements. Significant intensity variations are also observed for the C=O, NH, and CO_2^- bands. The amide C=O band at 1635 cm^{-1} and the NH at 3304 cm^{-1} are very strong in the bulk but are relatively weak or unobserved in the multilayer spectrum, both vibration modes being close to parallel to the surface. One of the most intense bands in the multilayer spectrum is that of the asymmetric carboxylate stretching at 1538 cm^{-1}, possibly superimposed on the NH_3^+ deformation band. A progression of five bands, separated by 20 cm^{-1} in the range 1150–1350 cm^{-1}, is attributed to the twist and wag modes of the methylene group and indicates an extended all-trans conformation of the polymethylene chain. Similar spectra were obtained with multilayers of **12** and **13**.

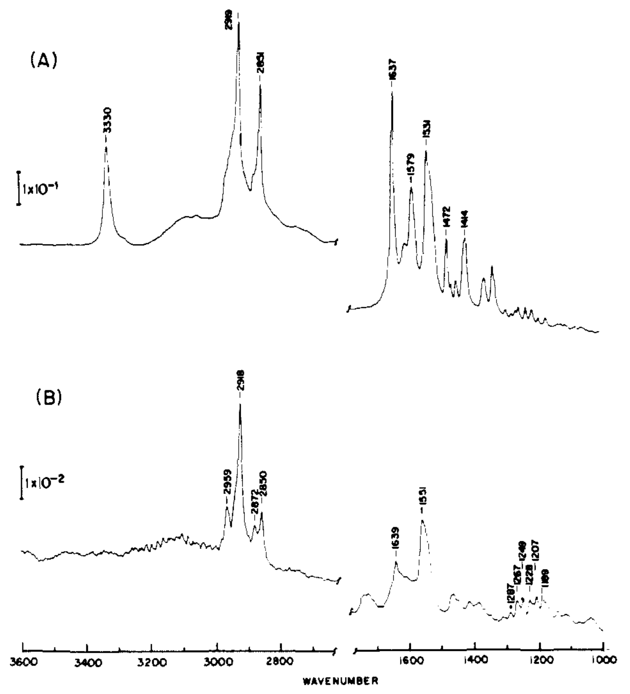

Figure 6. IR spectra of **1**: (A) in the bulk (KBr pellet); (B) in LB film (five layers).

The IR spectrum obtained for five Z-type layers of **1** shows the same features observed for compounds in class III (Figure 6), whereas the spectrum of five Y-type layers of **2** shows a relatively low intensity of the asymmetric CO_2^- stretching at 1558 cm^{-1} and strong symmetric CO_2^- at 1410 cm^{-1}. This observation indicates a somewhat different orientation of the CO_2^- groups of **1** and **2** relative to the surface (Figure 7).

Nine layers of **10** show a relative strong asymmetric CH_2 stretching mode, indicating some tilt of the chain. The ester carbonyl band at 1734 cm^{-1} implies a significant component perpendicular to the surface. The symmetric carboxylate band at 1416 cm^{-1} is relatively intense while the asymmetric carboxylate is absent. The strong absorption bands at 1241 and 1209 cm^{-1} are assigned to the C–O stretching vibration having a large contribution in the direction normal to the surface. No progression of bands in the region 1150–1350 cm^{-1} could be detected (Figure 8).

Second-Harmonic Generation (SHG). SHG is a process in which light at a frequency ω is (partially) converted into light at frequency 2ω. This process does not involve a specific molecular excitation, but rather arises from residual noncentrosymmetrical second-order polarizability. Therefore, SHG is a sensitive probe of acentric surface structures.[22] Within the electric dipole ap-

---

(20) Recent surface X-ray reflectivity measurements of one deposited layer of **15** on a glass slide gave a film thickness of 37.8 Å, which implies a tilt of 23°. Grayer Wolf, S. Private communication.

(21) (a) Allara, D. L.; Nuzzo, R. G. *Langmuir* **1985**, *1*, 52. (b) Gun, J.; Iscovici, R.; Sagiv, J. *J. Colloid Interface Sci.* **1984**, *101*, 201.

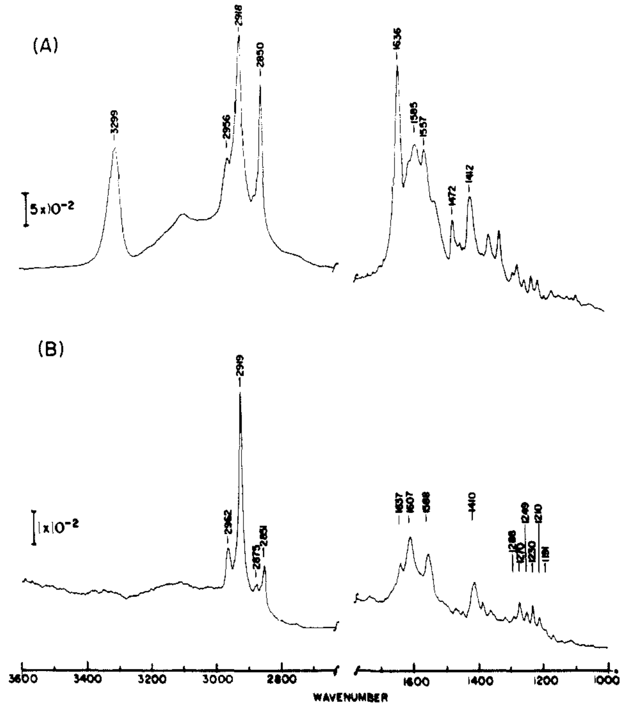

Figure 7. IR spectra of **2**: (A) in the bulk (KBr pellet); (B) in LB film (five layers).

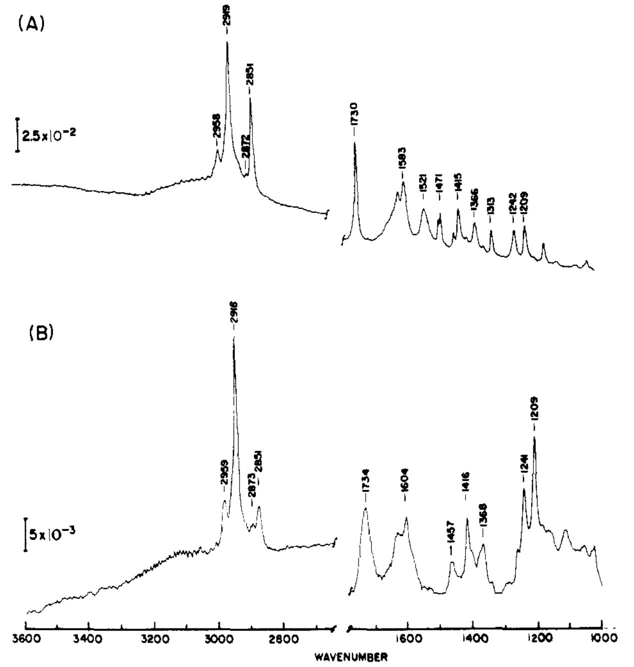

Figure 8. IR spectra of **10**: (A) in the bulk (KBr pellet); (B) in LB film (nine layers).

proximation, the SHG intensity from an N-layer LB film with thickness $\ll\lambda$ is

$$I_{2\omega} \propto |\hat{e}_{2\omega}\cdot\overleftrightarrow{\chi}_F^{(2)}\cdot\hat{e}_\omega\hat{e}_\omega|^2$$

where $\hat{e}_\omega$ and $\hat{e}_{2\omega}$ are the polarization vectors of the fundamental and second-harmonic waves, respectively. $\chi_F^{(2)}$, the net nonlinear susceptibility of the film, is obtained by tensorial summation of the contribution from each layer:

$$\overleftrightarrow{\chi}_F^{(2)} = \sum_{i=1}^{N}\overleftrightarrow{\chi}_i^{(2)}(2\omega = \omega + \omega)$$

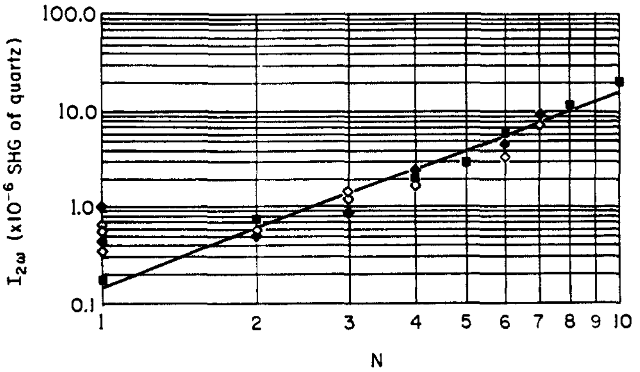

Figure 9. Intensity of second-harmonic light ($I_{2\omega}$) produced in LB films of compound **16** as a function of layer number (N). Both the fundamental and second-harmonic beams are p-polarized. Different symbols indicate films deposited at different times and/or troughs. The line (with slope 2) is the best fit according to the least-squares criterion.

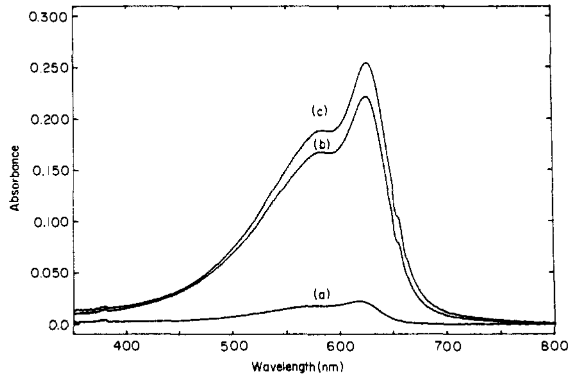

Figure 10. Absorption spectra of (a) 1, (b) 11, and (c) 13 layers of **23** polymerized at the air/water interface and transferred on glass slide.

The dependence of $I_{2\omega}$ on N is a critical test of film type. Constructive addition occurs in ideal X- or Z-type films, yielding N^2 dependence. In Y-type films, destructive interference between oppositely oriented layers causes complete cancellation (for even N) or a residual monolayer contribution (for odd N). Amphiphiles synthesized for SHG are listed in Table I under class IV. Compouds **16** and **17** showed long-term stability at the air/water interface, and multilayer films could be deposited without occurrence of monolayer collapse. Figure 9 shows $I_{2\omega}$ vs N for a number of mono- and multilayer samples of compound **16** prepared on glass slides at different times and with different LB troughs. The very good N^2 dependence is a direct proof of the formation of Z-type films. The long-term stability of these films has been demonstrated by reproducing the SHG measurements after 1 year from the date of sample preparation. Compared to the known value of the hyperpolarizability of *p*-nitroaniline (pNA), the SHG conversion efficiency is relatively low, indicating the *p*-nitroaniline chromophore in the LB films may have a rather large average tilt from the surface normal (approximately 70°).

Multilayers of compounds **19** and **20** were also studied by SHG. One would expect more efficient SHG from these films due to the larger molecular hyperpolarizability of the merocyanine chromophore than that of pNA. However, we observed a sublinear dependence of $I_{2\omega}$ on N for $N \leq 4$ and a saturation of the SHG signals for $N \geq 4$. UV-visible absorption spectra of these films indicated a substantial degree of protonation in the merocyanine moiety, which apparently caused the reduction in the molecular hyperpolarizability.[23] Monolayers of compounds **21** and **22** at the air/water interface were not sufficiently stable at constant surface pressures to allow multilayer deposition. But better stability was obtained in monolayers of binary mixtures of these amphiphiles with compound **13**. For example, we could prepare

---

(22) (a) Heinz, T. F.; Chen, C. K.; Ricard, D.; Shen, Y. R. *Phys. Rev. Lett.* **1982**, *48*, 478. (b) Rasing, T.; Berkovic, G.; Shen, Y. R.; Grubb, S. G.; Kim, M. W. *Chem. Phys. Lett.* **1986**, *130*, 1.

(23) Marowsky, G.; Chi, L. F.; Mobius, D.; Steinhoff, R.; Shen, R. Y.; Dorsch, D.; Rieger, B. *Chem. Phys. Lett.* **1988**, *147*, 420.

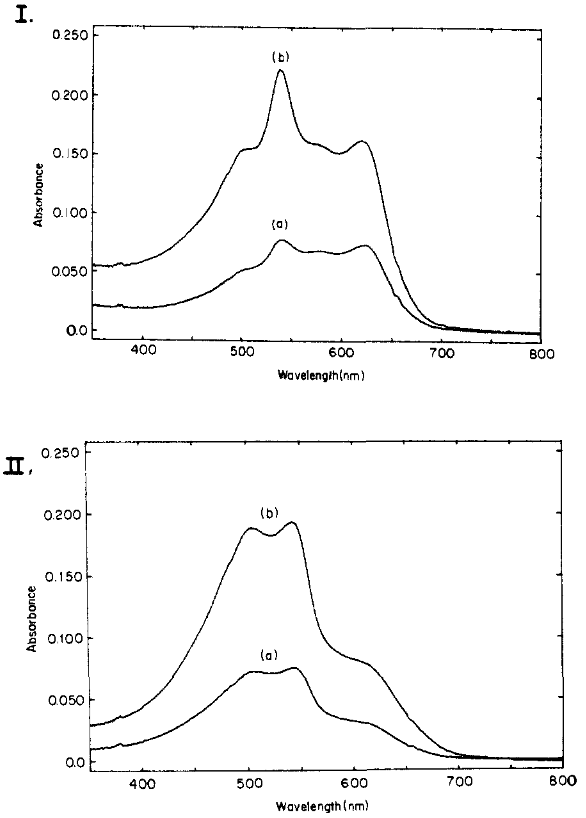

Figure 11. (I) Absorption spectra of (a) 12 and (b) 34 layers of **24** polymerized at the air/water interface and transferred on glass. (II) Same as (I) after treatment with $CHCl_3$.

Z-type films up to 12 layers thick by deposition of a 1:1 (molar ratio) monolayer mixture of **21** and **13**. These mixed multilayers also exhibit SHG. In this case there was substantial in-plane inhomogeneity, indicating clustering and domain formation to be active, but nevertheless allowing stable Z-type layer production.

UV-Visible Spectroscopy. The polydiacetylene multilayers of compounds **23** and **24** were characterized by UV-visible spectroscopy. Photopolymerization of **23** by UV light (254 nm) at the air/water interface or as a deposited monomeric multilayer gave a blue polymer (λ_{max} = 626 nm) as shown in Figure 10. This polymer did not undergo the usual "blue" to "red" transition on treatment with $CHCl_3$.[19a]

The photopolymer of **24** was purple (λ_{max} = 540, 620 nm), possibly a mixture of the blue and red forms. This polymer turned into the red form on treatment with $CHCl_3$ (Figure 11). This observation suggests a more ordered and stable structure for polymer **23**, perhaps due to the favorable hydrogen bonding between neighboring molecules in this monolayer. The red of polymer **24** may be a result of some strain in the polymer backbone, distorting the planar conformation.[24]

Discussion

A new class of amphiphilic molecules yielding stable Z-type LB films is described. We have found that amphiphiles with two amide groups in the hydrocarbon chain invariably form Z-type films. On the other hand, amphiphiles with one amide group in the chain form Y- or Z-type multilayers. The nature of the film depends upon the location of the amide group along the chain. Similar amphiphiles, where the amide group was replaced by an ester, behave as the regular hydrocarbons, yielding the nonpolar Y-type films. When polarizable groups such as *p*-nitroaniline were attached at the ω-position of the diamide amphiphiles, these compounds still preserved their property of deposition in Z-type mode, yielding multilayers displaying frequency doubling via second-harmonic generation. These nonlinear optical properties were still observed 1 year after deposition.

Wettability studies on deposited Z-type films (on hydrophilic or hydrophobic glass slides) indicate lower contact angles than those observed for regular hydrocarbons such as stearic acid. In the case of α-amino amphiphiles bearing two amide groups along the chain (yielding Z-type), the advancing contact angle is always lower than 90° and the receding contact angle lower than 45°, whereas in the case of amphiphiles bearing an ester group and in some cases an amide (yielding Y-type), the advancing water contact angle is larger than 90°. These contact angles determine the shape of the meniscus during the dipping cycle and thus the deposition mode.

The fact that wetting properties of the substrate or of the previously deposited layer are crucial in determining the mode of deposition is clear from the following observation: When deposition was made onto hydrophobic glass slides (treated with OTS, water contact angle 110°), all Z-type-forming compounds transferred first as a Y-type bilayer followed by Z-type multilayers. Furthermore, a monolayer of diamide **15** was deposited on a hydrophobic glass slide to form a Y-type bilayer, followed by eight Z-type layers. On top of this multilayer four layers of the ester **10** were transferred: the first was deposited in a Z-type mode, by virtue of the hydrophilic nature of the previously deposited layer, and the next three as Y-type structure, in keeping with the contact angle of the deposited ester. These layers were further covered with four layers of **15**: the first bilayer was Y-type, followed by two Z-type depositions.

The very low receding contact angles of these Z-type films indicate efficient water penetration and retention in the films that seem to be highly porous. Indirect support for the porous nature of these films comes from grazing angle X-ray diffraction and X-ray reflectivity measurement of **1** at the air/water interface at 20 mN/m. The diffraction data showed that this monolayer is a two-dimensional powder with a strong reflection corresponding to a *d* spacing of 4.53 Å and a coherence length of approximately 500 Å. The hydrocarbon chains in these domains are tilted at an angle of 30° to surface normal, thus precluding close packing of the neighboring domains.[25a] The reflectivity data indicated that the monolayer coverage at 20 mN/m is as low as 90%, thus exposing bare patches of water. A compressed monolayer of diamide **12** over water gave an X-ray diffraction peak at a *d* spacing of 4.5 Å, which suggests that the monolayer packs in a manner similar to that of palmitoyl-(*S*)-lysine (**1**).[25b] Thus, we propose that these films are porous and that water may penetrate therein. The amide groups located at various sites along the hydrophobic chains generate hydrophilic centers that may retain water molecules via hydrogen bonds. In addition, the hydrophilic head groups such as α-amino acids and carboxylic acids, which cannot form hydrogen-bonded pairs (in contrast to the Y-type), are free to bind water between the layers. We suggest that when these films are immersed in water, the voids between the domains retain water and the water contact angle is reduced to such an extent as to permit deposition of the next layer on the upstroke. Strong evidence for the role played by occluded water in determining the mode of deposition is obtained from the following experiments: A monolayer of **1** has an advancing contact angle of 80° and forms Z-type multilayer when deposited at a pressure of 20 mN/m, whereas at 30 mN/m the monolayer domains are more tightly packed, yielding a more hydrophobic surface (advancing contact angle of 85°) and Y-type deposition. Similarly, the occluded water could be removed by drying the monolayer of **1**, deposited at 20 mN/m, for 24 h at 25 °C in a desiccator. The resulting monolayer had a larger contact angle with water (89°), and consequently, the following layer gave Y-type deposition.

Finally, this proposed mechanism implies that it should hold also for amphiphilic molecules bearing other polar groups along

---

(24) Patel, G. N.; Chance, R. R.; Witt, J. D. *J. Chem. Phys.* **1979**, *70*, 4387.

(25) (a) Grayer Wolf, S.; Leiserowitz, L.; Lahav, M.; Deutsch, M.; Kjaer, K.; Als-Nielsen, J. *Nature* **1987**, *328*, 63. (b) The fact that crystalline order is maintained upon transfer to the glass slide is demonstrated by the grazing incidence diffraction peak at a *d* spacing of 4.5 Å from 13 layers of **10**.

Table II

no.	compound	multilayer type	contact angle advancing (receding)
25	$CH_3(CH_2)_5CH(OH)(CH_2)_{10}CO_2H$	Z	65 (<10)
26	$CH_3(CH_2)_5CH(OH)(CH_2)_{10}C(O)NH(CH_2)_2CH(NH_3^+)CO_2^-$	Z	68 (10)
27	$CH_3(CH_2)_5C(O)(CH_2)_{10}CO_2H$	Y	90 (20)
28	$CH_3(CH_2)_5C(O)(CH_2)_{10}C(O)NH(CH_2)_2CH(NH_3^+)CO_2^-$	Z	80 (25)

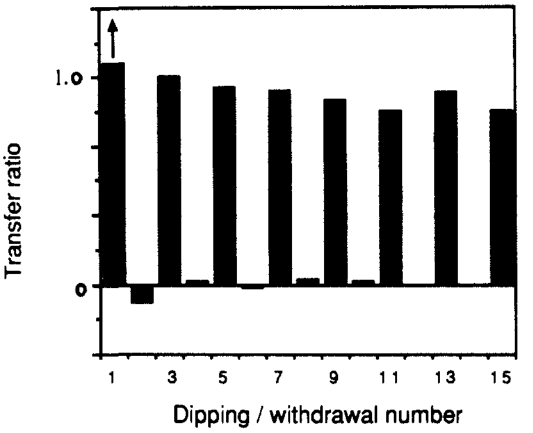

Figure 12. Histogram showing the apparent transfer ratio of a monolayer of **26** on hydrophilic glass slide.

the hydrocarbon chain. Thus, we expected that incorporation of hydroxyl groups should have a similar effect on wettability as the amides. The behavior of 12-hydroxystearic acid and 12-ketostearic acid at the air/water interface has been reported,[26] but to the best of our knowledge no multilayer formation from these compounds has been described. Thus, in contrast to stearic acid, we were able to deposit four Z-type layers of 12-hydroxystearic acid with good transfer ratios, but the monolayer was not stable enough to permit large number of depositions without collapse (Table II). Comparative measurements of water permeability of various monolayer films[27] showed that a hydroxyl group close to the center of the amphiphilic chain affected the packing of the molecules in such a way that the monolayer was highly permeable to water. The monolayer of compound **26**, synthesized by coupling 12-hydroxystearic acid with α,γ-diaminobutyric acid, showed increased stability at the air/water interface and was deposited in a Z-type fashion with transfer ratios of 1 ± 0.15 (Figure 12).

Incorporation of ketone groups along the hydrocarbon chain, as in 12-ketostearic acid, does not reduce the advancing contact angle with water below 90°; thus, Y-type deposition was obtained. The monolayer showed the same instability as 12-hydroxystearic acid. 12-Ketostearic acid was coupled with α,γ-diaminobutyric acid to yield compound **28** which formed a stable monolayer at the air/water interface and was deposited as a Z-type multilayer.

Incorporation of esters or ketones only, which bind water less firmly than amides or hydroxyls, did not reduce the advancing water contact angles below 90°; thus, the regular Y-type depositions were obtained.

Moreover, it seems that incorporation of various groups that are able to form hydrogen bonds between neighboring molecules in the domains also act as stabilizing functions and prevent any possible rearrangement of the deposited layers to the Y-type packing. This long-term stability was also demonstrated by an SHG study on the multilayers of **16**.

Successful design of Z-type multilayers requires a deep understanding of the wettability properties of the surfaces, on a molecular level, which obviously depends not only on the structured fraction of the films but also on their defect sites and porosity. In the absence of such knowledge, the empirical approach described here should be valid in the foreseeable future.

Experimental Section

Synthesis of Amphiphilic Molecules. Amphiphiles with α-amino acid or carboxylic acid head groups and one amide bond along the hydrocarbon chain were prepared by activation of the corresponding carboxylic acids via the succinimidyl ester and then reacted with the required amino acid. Amphiphiles with two amide bonds in the hydrocarbon chain were similarly prepared via the succinimidyl ester of the corresponding carboxylic acid coupled with the required ω-amino acid. The resulting acid was further activated and reacted with the desired α,ω-diamino carboxylic acid.

A. General Procedure for the Preparation of *N*-Hydroxysuccinimidyl Esters. Portions of 1 mmol of carboxylic acid, 1.1 mol *N*-hydroxysuccinimide, and 1.1 mmol dicyclohexylcarbodiimide (DCC) were dissolved in dry THF or CH_2Cl_2 (1 mL/mmol of reactant), and the resultant mixture was stirred for 1 h at 0 °C and overnight at room temperature. The precipitated dicyclohexylurea (DCU) was filtered, and the solution was concentrated to yield the crude active ester as crystalline material. If necessary, the ester was purified by column chromatography on silica gel with CH_2Cl_2 as eluent.

B. General Procedure for the Reaction of Succinimidyl Ester with ω-Amino Carboxylic Acids. Portions of 1 mmol of the corresponding active ester and ω-amino carboxylic acid were suspended in dry dioxane and stirred at 50–60 °C for 4 h. The hot reaction mixture was filtered, diluted with ice water to precipitate the product, and filtered. The product was purified by recrystallization from ethanol.

C. General Procedure for the Reaction of Succinimidyl Esters with α,ω-Diamino Carboxylic Acids.[28] A 1-mmol sample of active ester was suspended in 2 mL of acetone and the resultant mixture added to a solution of 1 mmol of α,ω-diamino carboxylic acid and 2 mmol of triethylamine in 2 mL of water. The reaction mixture was stirred vigorously for 4 h, then neutralized with acetic acid, and diluted with water. The precipitate was removed by filtration and washed with water, methanol, and CH_2Cl_2. Recrystallization from acetic acid or acetic acid/ethanol yielded the pure product.

The synthesis and characterization of compounds **1–5**, **10** and **11** are described in ref 18a.

Compound 6 was synthesized from undecanoic acid and 12-aminoundecanoic acid according to procedures A and B: mp 102–104 °C (methanol); IR (KBr) 3318, 2954, 2919, 2850, 1696, 1635, 1544, 1472 cm^{-1}; NMR ($CDCl_3$) δ 0.87 (br t, 3 H), 1.26 (m, 34 H), 2.20 (m, 4 H), 3.19 (m, 2 H), 5.6 (br s, 1 H). Anal. Calcd for $C_{23}H_{45}NO_3$: C, 72.01; H, 11.83; N, 3.65. Found: C, 71.93; H, 11.61; N, 3.94.

Compound 7. A 1-mmol sample of the succinimidyl ester of **6** was suspended in 3 mL of 25% aqueous NH_3 and the resultant mixture stirred for 18 h. Filtration yielded a colorless solid, which was recrystallized from ethanol: mp 140–142 °C; IR (KBr) 3401, 3332, 3198, 2920, 2851, 1646, 1637, 1532, 1472, 1422 cm^{-1}; NMR ($CDCl_3$) δ 0.87 (br t, 3 H), 1.26 (m, 34 H), 2.17 (m, 4 H), 3.20 (m, 2 H), 5.5 (br s, 1 H), 5.9 (br s, 2 H). Anal. Calcd for $C_{23}H_{46}N_2O_2$: C, 72.20; H, 12.12; N, 7.32. Found: C, 71.97; H, 12.12; N, 7.29.

Compound 8 was synthesized by coupling the succinimidyl ester of **9** with (*S*)-lysine according to procedures A and C: mp 232–236 °C (acetic acid); IR (KBr) 3328, 2919, 2852, 1736, 1640, 1581, 1531, 1471, 1416, 1179 cm^{-1}. Anal. Calcd for $C_{29}H_{56}N_2O_5$: C, 67.93; H, 11.01; N, 5.46. Found: C, 68.20; H, 10.84; N, 5.27.

Compound 9. A 15-mmol sample of undecanoic acid was added under nitrogen to a solution of 15 mmol *N,N*-carbonyldiimidazole in 30 mL of dry THF. The reaction mixture was stirred for 45 min at 25 °C and for 20 min at 45 °C until no further CO_2 evolution was observed. A 15-mmol portion of 12-hydroxydodecanoic acid was added, and the reaction mixture was refluxed for 2.5 h and left under nitrogen at room temperature overnight. Evaporation of the solvent gave an oil, which was dissolved in CH_2Cl_2, washed with water, dried, and evaporated to dryness. The product was crystallized from petroleum ether: mp 47–48 °C; IR (KBr) 3414, 2917, 2850, 1735, 1711, 1472, 1464, 1281, 1244, 1211, 1183 cm^{-1}; NMR ($CDCl_3$) δ 1.05 (br t, 3 H), 1.28 (m, 34 H), 2.30 (m, 4 H), 4.05 (br t, 2 H). Anal. Calcd for $C_{23}H_{44}O_4$: C, 71.83; H, 11.53. Found: C, 71.85; H, 11.50.

---

(26) Tachibana, T.; Yoshizumi, T.; Hori, K. *Bull. Chem. Soc. Jpn.* **1979**, *52*, 34.

(27) Walker, D. C. *Prepr.—Am. Chem. Soc., Div. Pet. Chem.* **1965**, *10*, D-61.

(28) Paquet, A. *Can. J. Chem.* **1976**, *54*, 733.

Compound 12 was synthesized by coupling the succinimidyl ester of **6** with (*S*)-lysine according to procedures A and C: mp 245–250 °C (acetic acid); IR (KBr) 3333, 2920, 2851, 1638, 1609, 1583, 1530, 1474, 1413, 1328 cm^{-1}; NMR (CF_3COOD) δ 0.89 (br t, 3 H), 1.1–2.6 (m, 40 H), 2.76 (m, 4 H), 3.60 (m, 4 H), 4.40 (m, 1 H). Anal. Calcd for $C_{29}H_{57}N_3O_4$: C, 68.05; H, 11.23, N, 8.21. Found: C, 68.16; H, 10.98; N, 7.77.

Compound 13 was synthesized from the succinimidyl ester of dodecanoic acid coupled with 11-aminoundecanoic acid according to procedures A and B. The resulting acid was further coupled with (*S*)-lysine through the succinimidyl ester according to A and C: mp 215–217 °C (acetic acid); IR (KBr) 3318, 2919, 2851, 1636, 1582, 1533, 1474, 1418 cm^{-1}; NMR (CF_3COOD) δ 1.04 (t, 3 H), 1.25–2.3 (m, 40 H), 2.9 (t, 4 H), 3.7 (4 H), 4.2 (t, 1 H).

Compound 14 was synthesized as **13** except for the last coupling step that was with (*S*)-ornithine: mp 208–210 °C (acetic acid); IR (KBr) 3304, 2921, 2851, 1635, 1605, 1576, 1538, 1471, 1418 cm^{-1}; NMR (CF_3COOD) δ 1.05 (t, 3 H), 1.3–2.3 (m, 38 H), 2.88 (t, 4 H), 3.8 (t, 4 H), 4.26 (t, 1 H).

Compound 15 was prepared from the succinimidyl ester of 11-bromoundecanoic acid and 12-aminododecanoic acid according to procedures A and B followed by coupling of the resulting acid with (*S*)-lysine according to A and C: mp 225–227 °C (acetic acid); IR (KBr) 3327, 2919, 2851, 1637, 1607, 1582, 1529, 1474, 1413, 1328 cm^{-1}; NMR (CF_3COOD) δ 1.1–2.6 (m, 40 H), 2.80 (m, 4 H), 3.5 (m, 6 H), 4.45 (m, 1 H). Anal. Calcd for $C_{29}H_{56}BrN_3O_4$: C, 58.96; H, 9.56; N, 7.11. Found: C, 59.27; H, 9.50; N, 6.71.

***N*-(4-Nitrophenyl)-12-aminododecanoic Acid.** A 71-mmol sample of KOH was dissolved in 70 mL of hot absolute ethanol. Portions of 35.5 mmol of 1-fluoro-4-nitrobenzene and 37.2 mmol of 12-aminododecanoic acid were added to the solution, and the solution was refluxed for 24 h. After the solution was cooled, the yellow precipitate was filtered, the filtrate was concentrated, and a second batch of yellow precipitate was obtained. It was combined with the first crop, and they were washed with CH_2Cl_2. The precipitate was dissolved in hot water, neutralized with 5 N HCl, and filtered to yield 65% product: mp 135 °C; IR (KBr) 3365, 2921, 2852, 1724, 1604, 1464, 1311, 1276, 1163, 1116 cm^{-1}; NMR ($CDCl_3$, Me_2SO-d_6) δ 1.28 (m, 18 H), 2.21 (br t, 2 H), 2.57 (br t, 2 H), 6.0 (br s, 2 H), AB (δ_A 6.56, δ_B 7.97, J = 9.3 Hz, 4 H).

Compound 16 was prepared by coupling **21** with (*S*)-lysine according to procedures A and C: mp 236–239 °C (acetic acid/water); IR (KBr) 3327, 2920, 2851, 1637, 1602, 1527, 1472, 1323, 1304, 1111 cm^{-1}; NMR (CF_3COOD) δ 1.3–2.4 (m, 44 H), 2.9 (t, 4 H), 3.7 (t, 6 H), 4.2 (t, 1 H), AB (δ_A 8.01, δ_B 8.67, J = 8.8 Hz, 4 H). Anal. Calcd for $C_{36}H_{63}N_5O_6$: C, 65.32; H, 9.59; N, 10.58. Found: C, 65.02; H, 9.70; N, 10.32.

Compound 17 was prepared by coupling **21** with (*S*)-ornithine according to procedures A and C: mp 194–196 °C; IR (KBr) 3380, 3310, 3047, 2922, 2851, 1639, 1603, 1540, 1506, 1469, 1319, 1306, 1111 cm^{-1}; NMR (CF_3COOD) δ 1.3–2.3 (m, 42 H), 2.5–2.9 (m, 4 H), 3.5–3.7 (m, 4 H), 4.9 (m, 1 H), AB (δ_A 7.9, δ_B 8.57, J = 8.7 Hz, 4 H).

Compound 18 was prepared by coupling *p*-nitrocinnamic acid with 12-aminododecanoic acid according to procedures A and B, followed by reaction of the resulting acid with (*S*)-lysine as in procedures A and C: mp 185 °C dec; IR (KBr) 3313, 3077, 2921, 2851, 1640, 1623, 1543, 1521, 1469, 1443, 1412, 1345, 1225 cm^{-1}; NMR (Me_2SO-d_6) δ 1.17–1.77 (m, 24 H), 3.25 (m, 2 H), 3.38 (t, 2 H), 3.48 (m, 2 H), 4.1 (m, 1 H), AB (δ_A 6.8, δ_B 7.55, J = 15.2 Hz, 2 H), AB (δ_A 7.84, δ_B 8.28, J = 8.9 Hz, 4 H).

***N*-(1-Oxo-11-iodoundecyl)-12-aminoundecanoic acid** was prepared from 11-iodoundecanoic acid[29] and 12-aminoundecanoic acid according to procedures A and B: mp 107–110 °C (methanol); IR (KBr) 3310, 2920, 2850, 1695, 1635, 1535 cm^{-1}; NMR ($CDCl_3$) δ 1.28 (m, 34 H), 2.17 (m, 4 H), 3.18 (br t, 4 H), 5.4 (br s, 1 H).

Compound 19. A solution of 3.44 mmol of γ-picoline and 3.36 mmol of *N*-(1-oxo-11-iodoundecyl)-12-aminododecanoic acid in 10 mL of isopropyl alcohol was refluxed for 16 h. After the solution was cooled, the precipitate was collected by filtration and crystallized from ethanol to yield colorless crystals (79%). A solution of these crystals, 3.36 mmol of 4-hydroxybenzaldehyde, and 0.3 mL of piperidine was refluxed 20 mL of ethanol for 17 h. After the solution was cooled, the red precipitate was filtered, suspended in 45 mL of aqueous 0.2 M KOH, and stirred at 50–60 °C for 30 min. The resulting crystals were isolated by filtration, dissolved in hot methanol, and crystallized again by adding water to yield 58% of red crystals: mp 225–235 °C; IR (KBr) 3312, 2919, 2851, 1643, 1623, 1601, 1558, 1521, 1470, 1286, 1171 cm^{-1}; NMR (Me_2SO-d_6) δ 1.1–2.1 (m, 34 H), 2.15 (br t, 4 H), 3.14 (br t, 2 H), 4.48 (br t, 2 H), AB (δ_A 6.85, δ_B 7.60, J = 8.6 Hz, 4 H), AB (δ_A 7.18, δ_B 7.85, J = 16.3 Hz, 2 H), AB (δ_A 8.05, δ_B 8.69, J = 6.9 Hz, 4 H).

***N*-(1-Oxo-11-bromoundecyl)-12-aminododecanoic acid** was prepared by coupling 11-bromoundecanoic acid[30] with 12-aminododecanoic acid according to procedures A and B: mp 122 °C (methanol); IR (KBr) 3313, 2920, 2879, 2852, 1696, 1634, 1536, 1472, 1414, 1228 cm^{-1}; NMR ($CDCl_3$) δ 1.28 (m, 34 H), 2.25 (m, 4 H), 3.23 (m, 2 H), 3.40 (t, 2 H), 5.3 (br s, 1 H). Anal. Calcd for $C_{23}H_{44}BrNO_3$: C, 59.73; H, 9.59; N, 3.03. Found: C, 60.07; H, 9.64; N, 3.28.

[^{13}N]-***N*-(1-Oxo-11-bromoundecyl)-1-(pentylamino)-1-oxo-12-aminododecane** was prepared by coupling *N*-(1-oxo-11-bromoundecyl)-12-aminododecanoic acid with pentylamine according to procedures A and B: mp 109–116 °C (ethanol/water); IR (KBr) 3317, 2921, 2851, 2811, 1638, 1541, 1468, 1437, 1423, 1383 cm^{-1}; NMR ($CDCl_3$) δ 0.89 (br t, 3 H), 1.27 (m, 40 H), 2.11 (m, 4 H), 3.28 (m, 6 H), 5.5 (br s, 2 H).

Compound 20. A solution of 2.04 mmol of γ-picoline and 1.43 mmol of [^{13}N]-*N*-(1-oxo-11-bromoundecyl)-1-(pentylamino)-1-oxo-12-aminododecane was stirred for 4 h at 140 °C. The resulting black oil was dissolved in a small amount of ethanol. When boiling acetone was added and the solution cooled, violet crystals were obtained (49%). A solution of 0.9 mmol of these crystals and 0.1 mL of piperidine in 10 mL of ethanol was refluxed for 16 h. After the solution was cooled, dark red crystals were obtained, which were suspended in 8 mL of 0.2 M KOH and stirred at 50–60 °C for 40 min. The crystals were filtered, washed with water and acetone, dried under vacuum, and purified by neutral aluminum oxide column chromatography with methanol/concentrated aqueous NH_3 (100/1) and recrystallized from methanol/acetone: IR (KBr) 3307, 2921, 2851, 1640, 1559, 1504, 1468, 1441, 1320, 1147 cm^{-1}; NMR (CD_3OD) δ 0.9 (br t, 3 H), 1.29 (m, 40 H), 2.10 (m, 4 H), 3.14 (br t, 4 H), 4.32 (m, 2 H), AB (δ_A 6.6, δ_B 7.42, J = 8.7 Hz, 4 H), AB (δ_A 6.85, δ_B 7.75, J = 15.8 Hz, 2 H), AB (δ_A 7.79, δ_B = 8.39, J = 6.7 Hz, 4 H).

Compound 21 was synthesized by coupling *N*-(4-nitrophenyl)-12-aminododecanoic acid with 12-aminododecanoic acid according to procedures A and B: mp 135–136 °C (methanol); IR (KBr) 3371, 3323, 2920, 2851, 1640, 1604, 1534, 1469, 1321, 1307, 1278, 1115 cm^{-1}; NMR ($CDCl_3$, Me_2SO-d_6) δ 1.27 (m, 36 H), 2.16 (m, 4 H), 3.17 (m, 4 H), 5.8 (br s, 1 H), 6.5 (br s, 1 H), AB (δ_A 6.54, δ_B 8.02, J = 9.4 Hz). Anal. Calcd for $C_{30}H_{51}N_3O_5$: C, 67.51; H, 9.63; N, 7.87. Found: C, 67.50; H, 9.68; N, 8.12.

Compound 22 was synthesized by coupling *N*-(4-nitrophenyl)-12-aminododecanoic acid with 12-aminododecane as in procedures A and B: mp 85–87 °C; IR (KBr) 3299, 2918, 2851, 1654, 1627, 1603, 1542, 1470, 1317, 1111 cm^{-1}; NMR ($CDCl_3$) δ 0.85 (t, 3 H), 1.26 (m, 38 H), 2.14 (m, 2 H), 3.18 (t, 4 H), AB (δ_A 6.52, δ_B 8.10, J = 8.8 Hz, 4 H).

Compound 23 was synthesized by coupling 10,12-nonacosadiynoic acid[49a] with (*S*)-lysine according to procedures A and C: IR (KBr) 3300, 2934, 2918, 2848, 1637, 1611, 1582, 1544, 1466, 1411 cm^{-1}; NMR ($CDCl_3$, CF_3COOD) δ 0.85 (t, 3 H), 1.3–1.6 (m, 44 H), 2.1–2.4 (m, 8 H), 3.3 (m, 2 H), 4.15 (m, 1 H).

Compound 24 was prepared by coupling 10,12-nonacosadiynoic acid[49a] with (*S*)-ornithine according to procedures A and C. IR (KBr) 3289, 2955, 2919, 2849, 1639, 1608, 1577, 1560, 1472, 1418 cm^{-1}; NMR (CF_3COOD) δ 0.93 (t, 3 H), 1.2–1.5 (m, 44 H), 2.1–2.3 (m, 6 H), 2.6 (m, 2 H), 3.7 (m, 1 H).

Compound 26 was prepared from *R*,*S*-12-hydroxystearic acid (**25**) (Aldrich, 97%) by oxidation with Jones reagent.

Compound 27 was synthesized by coupling of succinimidyl ester of *R*,*S*-12-hydroxystearic acid with α,γ-diaminobutyric acid according to procedures A and C: IR (KBr) 3347, 2955, 2923, 2850, 1687, 1647, 1586, 1560, 1548, 1466, 1411, 1095, 1077 cm^{-1}; NMR (CF_3COOD) δ 0.93 (br t, 3 H), 1.2–1.8 (m, 28 H), 2.5–2.9 (m, 4 H), 3.8 (m, 1 H), 4.9–5.2 (m, 1 H).

Compound 28 was synthesized by coupling succinimidyl ester of 12-ketostearic acid with α,γ-diaminobutyric acid according to procedures A and C: IR (KBr) 3330, 2956, 2917, 2851, 1701, 1639, 1605, 1583, 1532, 1471, 1443, 1416, 1384, 1330 cm^{-1}.

IR spectra were measured on a FT-IR Nicolet MX-1 spectrometer; NMR spectra were measured on Varian FT-80A or Bruker WH-270 NMR spectrometers. UV spectra were measured on a Hewlett-Packard 8450A diode array spectrophotometer.

Substrates. Glass slides (Gebruder Rettberg GmbH) were used as substrates for study of deposition behaviors and for contact angle measurements. These slides were placed in a Teflon holder and cleaned thoroughly according to the procedure described in ref 31. Glass slides were made hydrophobic by reaction with octadecyltrichlorosilane (OTS).[31]

Substrates for IR-RA and ellipsometric measurements were glass slides coated with 50 Å of TiO_2 and 1000 Å of Au (Evaporated Metal

---

(29) Ashton, R.; Smith, J. C. *J. Chem. Soc.* **1934**, 1308.

(30) Jones, R. G. *J. Am. Chem. Soc.* **1947**, *69*, 2350.

(31) Maoz, R.; Sagiv, J. *J. Colloid Interface Sci.* **1984**, *100*, 465.

Films). These substrates were thoroughly cleaned by soxhlet extraction with *n*-hexane for several hours, followed by argon plasma cleaning for 15 min (Harrick PDC-3XG Plasma Cleaner). Optical parameters of the bare substrate were measured within 15 min after cleaning. IR spectrum of the bare substrate was used as reference and was measured within 1 h after cleaning.

Pressure–area isotherms and deposition experiments were performed on a computer-controlled Lauda film balance, placed in a laminar flow hood, and thermostated to 20 °C. Dipping and withdrawal rate of substrates was 1 cm/min, with a drying time of 5 min after each cycle. Samples of 0.1–0.7 mL of 10^{-4}–10^{-3} M solutions of the amphiphiles in chloroform/trifluoroacetic acid (95/5) or in chloroform/methanol (85/15) were used as spreading solutions. Double-distilled water (Corning Mega-Pure System MP-6A) was used as subphase for all experiments. Compressed monolayer films were stabilized for $^1/_2$ h at constant pressure of 20 mN/m before depositions were initiated.

Contact Angles were measured by the sessile drop method, with a Rame–Hart contact angle goniometer. Contact angles were measured $^1/_2$ h after film deposition and were remeasured after 24 h. Static advancing contact angles were measured by applying a drop on the surface with a micrometer syringe, and receding contact angles were measured by reducing the volume of the drop until the periphery of the drop retreated. Readings were taken approximatly 30 s after the drop was applied at three different positions along the substrate, and the precision is ±2°.

Second-harmonic generation (SHG) tests were performed by a weakly focused Q-switched Nd:YAG laser with the following characteristics: wavelength ($\lambda = 2\pi c/\omega$) 1.06 μm, pulse width ≈8 ns, pulse energy <40 mJ, beam size at the sample ≈2.4 mm (diameter). The second-harmonic radiation at 532 nm was detected in the 45° transmission geometry through a high-f-number, spectrally filtered, high-efficiency collection system. This system provides substantial discrimination against incoherent emission and scattered radiation. Polarization control devices are located in the laser and detection branches. The samples are mounted on rotation/translation stages, which allow us to test the anisotropy of the samples' SHG properties. SHG intensities are measured relative to the SHG of quartz.

IR-RA measurements were taken with a FT-IR Nicolet-MX-1 spectrophotometer with a Harrick ATR attachment set at 75° incidence and Harrick Brewster angle Ge polarizer. Details of the optical set up used are described in ref 21b.

Ellipsometric measurements were performed on a Rudolph Research AutoEL-IV ellipsometer. The Auto-EL-IV is a microcomputer-controlled automatic-nulling ellipsometer. From the measured azimuths of polarizer and analyzer, the instrument computes two intermediate parameters, Δ and ψ, which are then used to calculate the optical constants of bare surfaces and the thickness of transparent films on these surfaces. Measurements were performed at 633 nm with a tungsten–halogen lamp; the angle of incidence was 70°, and the refractive index used for the calculations was 1.45. The average value of at least three measurements, taken at different points along the substrate, was used for the calculations.

Low-angle X-ray diffraction was performed on a Rigaku powder diffractometer with a thin film attachment, with Cu Kα radiation (λ = 1.54 Å).

Acknowledgment. We thank Dr. J. van Mil for performing the X-ray measurements, Drs. E. Landau and G. Berkovic for discussions, and Yeda preindustrial funds for financial support. K.H. thanks the Max-Planck-Gesellschaft for a Minerva fellowship.

Generation of Alkyl Carbanions in the Gas Phase

Susan T. Graul[†] **and Robert R. Squires**[*]

Contribution from the Department of Chemistry, Purdue University, West Lafayette, Indiana 47907. *Received August 18, 1989*

Abstract: The scope and limitations of collision-induced decarboxylation of carboxylate negative ions as a method for generating gas-phase carbanions are described. Simple alkyl carbanions can be observed as fragments from a variety of aliphatic carboxylates, provided only that the carbanion has a lifetime toward electron detachment greater than ~25 μs. Several heretofore unknown alkyl carbanions have been observed, including the neopentyl anion, the 2- and 3-methylbutyl anions, cyclopentylmethyl anion, and cyclohexylmethyl anion, as well as cyclic and polycyclic carbanions such as the 1- and 2-methylcyclopropyl anions and the 1-bicyclopentyl anion. An empirical correlation between the electron affinities of primary alkyl radicals (RCH_2) and the analogous alkoxyl radicals (RO) is described that correctly predicts the stability and detectability of the corresponding primary carbanion fragments (RCH_2^-) from collision-induced decarboxylation. A number of α-substituted methyl anions and β-substituted ethyl anions have been formed by this method; both familiar and novel examples of these types of carbanions are described. The competing higher energy fragmentations and low-energy reactions of collisionally activated carboxylate ions are also discussed, including β-radical cleavages, remote-site fragmentations, and intramolecular isomerizations that occur prior to dissociation.

Carbanions play a central role in organic and organometallic chemistry because of their widespread synthetic utility in carbon–carbon and carbon–metal bond formation reactions.[1-5] For synthetic chemists, the isolated carbanion serves as a convenient "synthon", or idealized fragment, that assists in the design of synthetic procedures and permits description of reaction mechanisms in straightforward terms.[6,7] However, it is widely recognized that in solution the actual reactive anionic species are not free carbanions, but are closely associated with and stabilized by counterions and solvent molecules, and further may exist as aggregates.[1-6,8,9] Accordingly, a detailed understanding of the intrinsic properties and reactivities of isolated carbanions, along with the changes that accompany ion pairing, solvation, and aggregation, is an important goal of carbanion research.

Studies of the chemistry and properties of carbanions in the gas phase provide the means to probe the intrinsic reactivity of these species and reveal the often dominating influence of the reaction medium on carbanion chemistry in solution. Although a great deal of information has been amassed from experimental studies for a wide variety of organic ions in the gas phase, as yet

---

[†] Present address: Department of Chemistry, University of California, Santa Barbara, CA 93106.

(1) Cram, D. J. *Fundamentals of Carbanion Chemistry*; Academic Press: New York, 1965.

(2) Buncel, E. *Carbanions: Mechanistic and Isotopic Aspects*; Elsevier: Amsterdam, 1975.

(3) Buncel, E., Durst, T., Eds. *Comprehensive Carbanion Chemistry. Part A: Structure and Reactivity*; Elsevier: Amsterdam, 1980.

(4) Bates, R. B.; Ogle, C. A. *Carbanion Chemistry*; Springer-Verlag: Berlin, 1983.

(5) Hartley, F., Patai, S., Eds. *The Chemistry of the Carbon–Metal Bond*; Wiley-Interscience: New York, 1985; Vols. 1 and 2.

(6) Stowell, J. C. *Carbanions in Organic Synthesis*; Wiley-Interscience: New York, 1979.

(7) Warren, S. *Organic Synthesis: The Disconnection Approach*; John Wiley & Sons: Chichester, U.K., 1982.

(8) Staley, S. W.; Dustman, C. K. In *Reactive Intermediates*; Jones, M., Moss, R. A., Eds.; John Wiley & Sons: New York, 1982; Vol. 2.

(9) Schleyer, P. v. R. *Pure Appl. Chem.* **1983**, *55*, 355.

0002-7863/90/1512-2506$02.50/0